

Assessment of an intermediate reprojection technique transitioning from planar to SPECT radionuclide ventriculography

Jim O'Doherty, CSci, PhD,^a Bruno Rojas Fisher, CSci, MSc,^b Jonathan Mark Price, MSc,^{c,b} and Kshama Wechalekar, MBBS, DRM, DNB (Nuclear Medicine)^b

^a PET Imaging Centre, Division of Imaging Sciences and Biomedical Engineering, King's College London, King's Health Partners, St. Thomas' Hospital, London, United Kingdom

^b Department of Nuclear Medicine, Royal Brompton Hospital, London, United Kingdom

^c Cancer Research UK and EPSRC Cancer Imaging Centre, Division of Radiotherapy and Imaging, Institute of Cancer Research, Sutton, United Kingdom

Received Jan 8, 2014; accepted May 2, 2014

doi:10.1007/s12350-014-9945-x

Background. The technique of SPECT-RNV (radionuclide ventriculography) offers a greater amount of clinically usable data than its planar counterpart (P-RNV). In transitioning from planar to SPECT-only acquisition methodologies, reprojection of the SPECT data can provide a planar dataset which can be used as an interim technique. The aim of this study was to test if reprojected planar images could be used as a surrogate for true planar images in SPECT-only setting.

Methods. We performed SPECT-RNV and P-RNV on 47 patients on traditional sodium iodide (NaI) cameras, determining left ventricular ejection fractions (LVEF) for planar (EF_P) and SPECT (EF_S) techniques. We reprojected the SPECT-RNV data along the best septal separation angle determined from planar scanning. This creates a further planar dataset denoted 'reprojected P-RNV' (rP-RNV) giving a reprojected ejection fraction (EF_R) which can be used as a validation variable in transitioning to SPECT-only acquisition.

Results. Performing *t* tests showed no statistical difference between EF_P and EF_R ($P > .017$) but bias was observed in EF_S results compared to EF_P and EF_S compared to EF_R results. An unblinded, comparison of parametric data between the three datasets for a subset of ten patients showed good clinical concordance. False negative and false positive rates were low for rP-RNV compared to P-RNV.

Conclusions. The reprojected planar LVEF correlates well to P-RNV EF values. The rP-RNV dataset can aid clinicians in transitioning from planar RNV to SPECT-only acquisition. (J Nucl Cardiol 2014;21:944–53.)

Key Words: Radionuclide angiography • left ventricular function • ejection fraction gated SPECT

INTRODUCTION

Left ventricular angiography was the clinical 'gold standard' for reliable and reproducible left ventricular

ejection fraction (LVEF) measurements¹ although owing to its invasive nature, it was not used frequently. Planar radionuclide ventriculography (P-RNV) is considered to be the imaging 'gold standard' for quantifying LVEF, attributed to its clinical use since the 1970s.^{2,3} The emergence of cardiac magnetic resonance imaging (C-MRI) has also shown strong promise at providing an alternative to radionuclide imaging, with excellent correlation between P-RNV and C-MRI LVEF values.⁴

Reprint requests: Jim O'Doherty, CSci, PhD, PET Imaging Centre, Division of Imaging Sciences and Biomedical Engineering, King's College London, King's Health Partners, St. Thomas' Hospital, London SE1 7EH, United Kingdom; jim.odoherty@kcl.ac.uk
1071-3581/\$34.00

Copyright © 2014 American Society of Nuclear Cardiology.

P-RNV finds many uses such as cardiac risk stratification, pre-chemotherapy cardiac function evaluation, congestive heart failure assessment, ischaemic heart disease and thus provides useful prognostic indicators.⁵

Disadvantages of planar RNV include reduced contrast, loss of depth perception, attenuation from overlying tissues and guesswork about best septal separation angle while setting the acquisition. These limitations of planar left anterior oblique (LAO) projection imaging have been well documented and highlighted again in a recent editorial.⁶ The effects include overlap of adjacent cardiac/lung structures and imprecise localisation of left ventricle (LV) and right ventricle (RV) abnormalities. The partial inclusion of the left atrium in the left ventricular ROI has previously been shown to decrease LVEF as a result of the left atrial counts from the filled left atrium contributing to the LV ROI at end-systole (the left atrium and LV beat out of phase with each other).⁷ Further issues include better LV function at higher LVEF with a smaller end-systolic volume (ESV), whereby the relative contribution from the left atrium becomes more significant. P-RNV at a traditional single LAO acquisition is also unable to assess motion in a direction perpendicular to the detector head. Although a caudal-cephalic tilt has been suggested to help define the valve plane and thus separate the LV from the left atrium,⁷ guidance on its use is minimal^{8,9} and availability of such a function on modern gamma cameras is becoming rare in the age of tomographic imaging.

SPECT-RNV overcomes many limitations of conventional P-RNV. The tomographic perspective improves separation of cardiac structures and three-dimensional information may improve the assessment of regional wall motion (RWM), the analysis of which is an important tool when evaluating cardiac function.¹⁰ Also, due to volumetric segmentation there is no need for a background correction and identification of septal separation angles. True assessments of LV volume are also attainable rather than the approximate assessment made by P-RNV. Issues of longer acquisition times, larger datasets, and inaccurate endocardial volume fitting algorithms have largely been addressed^{11,12} and automated algorithms commercially available to calculate LVEF have been extensively validated.¹³ Phantom studies have also validated the use of gated SPECT-RNV software against a dynamic three-dimensional biventricular phantom.¹⁴

LVEF values determined by SPECT-RNV and P-RNV have been compared in a number of studies showing moderate to excellent correlation between LVEF determined by both methods on a range of patient cohorts (0.92,¹⁵ 0.9,¹⁰ 0.89⁷ and 0.78¹⁶). All of these studies show a systematic positive bias towards

SPECT-RNV LVEF ranging from 2.8% to 10% through the use of a variety of software packages indicating that the bias effect is software independent. In a study of 23 patients SPECT-RNV EF were consistently higher than those determined by P-RNV, caused by an overlap in the left atrium in the planar image being removed during SPECT imaging.⁷ This was determined by reprojecting the SPECT-RNV back to a conventional LAO projection with and without masking of the left atrium, which showed that reprojected LVEF (excluding the left atrium) were greater than planar LVEF by a factor of 1.4.

A single study comparing LV volume compared to that determined by invasive x-ray angiography found good correlation 0.83-0.86,¹² although they found that SPECT results were consistently underestimated. The same study compared LVEF between four software packages to P-RNV and observed good correlation (0.98-0.99) for three of the four packages. Other research has shown a good correlation between software packages for LV parameters but extreme variability for RV parameters.¹⁵ They also showed that RWM may be better assessed through the use of cine displays available only from tomographic imaging. Other work examining SPECT and planar LVEF differences on a large cohort of patients ($n = 5,558$) concluded that they compared well to each other ($r = 0.94$), and also to echocardiography and angiography results.¹⁶

A possible solution to the lack of impetus in transitioning to SPECT imaging is to present reporting clinicians with both P-RNV and SPECT-RNV images. Given that variables determined by P-RNV in some cases can be different from those determined by SPECT-RNV, the techniques should not be used interchangeably. Instead of acquiring both datasets sequentially (which may take up to an hour), it is possible to reproject the SPECT data into a pseudo-planar dataset thereby producing both datasets from a single SPECT scan. When a site is shifting from P-RNV to SPECT-RNV, it may be desirable to have both types of imaging for comparison and also provides good learning experience for reporting clinicians. Thus extracting a reprojected planar dataset (rP-RNV) from the SPECT-RNV data, without the need for additional imaging can help the clinicians to see familiar planar-like images during the transition and the rP-RNV EF can be used as a check for the EF provided by SPECT-RNV dataset. This technique has been advocated by a recent editorial⁶ and recent research examining reprojection of SPECT-RNV data has compared P-RNV from two traditional sodium iodide (NaI) gamma camera systems (one general and one cardiac specific) against a reprojected SPECT derived from a dedicated CZT cardiac gamma camera. Their results show a correlation of $r > 0.94$

between LVEF when processed by the same analysis software.¹⁷ Their work was aimed at providing backward compatible capability between new modern solid-state gamma cameras and NaI cameras. Given that in order to monitor cardiotoxicity, patients may be imaged periodically over a long-time frame and thus a consistent value of EF is of paramount importance in ongoing prognosis regardless of the employed imaging hardware.

This work examines the LVEF between datasets acquired from P-RNV and SPECT-RNV acquired sequentially on the same traditional NaI gamma camera, while also reprojecting the SPECT dataset along the P-RNV projection angle to provide a third dataset to enable a transition from P-RNV to SPECT-RNV only.

METHODS

Gamma Cameras

Two traditional NaI gamma cameras were used in this study, a GE Infinia Hawkeye and an ADAC Forte. The technical parameters of both cameras and collimators are detailed in Table 1.

Patients

Fifty patients were selected (22 men, 28 women, mean age of 57 and a range of 18-81 years), referred for a range of clinical indications (40 during monoclonal antibody trastuzumab—Herceptin—treatment or anthracyclines, three for assessment prior to cardiac resynchronisation therapy, five with atrial fibrillation and two for baseline LV function assessment). All patients consented to both SPECT-RNV and P-RNV imaging. Each patient underwent in vivo blood labelling by 0.03 mL·kg⁻¹ stannous fluoride made up with 6 mL 0.9% saline, followed 20 minutes later by an intravenous

Table 1. Parameters for both gamma cameras used in the study

	GE Infinia	ADAC Forte
Collimator	LEHR	VXGP
Crystal	3/8" NaI	5/8" NaI
Resolution (mm) @ 10 cm	7.4	8.0
Sensitivity (cps·MBq ⁻¹)	72.1	88.0
SPECT pixel size (mm)	6.799	6.334
Planar pixel size (mm)	4.420	4.223
Zoom (planar)	2.0	2.19
Zoom (SPECT)	1.3	1.46

Collimators were chosen to offer similar performance of cameras.

injection of approximately 800 MBq of ^{99m}TcO₄⁻. Three patients were excluded from the study (2 Herceptin, 1 AF) due to technical issues with image processing, thus the study consisted of data from 47 patients. A nuclear medicine physician, experienced with planar and SPECT-RNV techniques, carried out all image processing on anonymised image datasets whilst blinded to the EF results from other techniques in order to remove any possible bias in results.

SPECT-RNV Image Acquisition

SPECT-RNV imaging was performed immediately post-injection, with collimators oriented at 90°. Patients were connected to a 3-point ECG lead with arms raised. Imaging on both cameras was acquired using 16 frames for 60 seconds per projection (30 projections) using a 64 × 64 matrix over a 180° arc (6° steps). SPECT-RNV imaging was performed using a zoom of 1.3 and 1.46 with resulting pixel sizes of 6.80 and 6.33 mm on Infinia and ADAC cameras, respectively. These pixel sizes are similar to those reported in other work acquiring SPECT-RNV on traditional gamma cameras.¹² Tomographic data were reconstructed using the Hermes Ordered Subset Expectation Maximisation (HOSEM©) algorithm; four iterations of ten subsets, Gaussian filter (order 5, 0.7 cycles·cm⁻¹), without attenuation correction or scatter correction.

SPECT-RNV Analysis: QBS Software

All SPECT-RNV analysis was carried out using Quantitative Blood Pool SPECT (QBS v2008, Cedars Sinai, USA) software, which automatically determines the left and right endocardial surfaces. First, the mitral valve plane and the interventricular septum are identified. We then used a combined count and volumetric-based segmentation method, which has been noted as a more favourable method than using volume of the region only.¹¹

The LV cavity at end-diastole is delineated by segmentation using an iterative threshold technique. The optimal threshold is reached when the resulting isocontour best fits the first derivative of the end-diastolic count distribution in all three dimensions. This threshold is then subsequently used to delineate the ventricle in the other time bins. There is scope for manual adjustment through the use of segmentation handles in the software. An experienced nuclear medicine physician adjusted the volumes where deemed necessary. Adjusted SPECT-RNV ejection fraction values (EF_S) were reported for each patient.

P-RNV Image Acquisition

Immediately following SPECT-RNV, P-RNV was carried out using the SPECT data to identify the angle of best septal separation. This was confirmed prior to imaging by identification on the patient positioning monitor. The patient remained on the scanning bed, in the same position as from SPECT-RNV imaging. Planar image acquisition conformed to EANM guidelines,⁹ namely 16 frames/R-R with a tolerance window of 10%, a matrix of 64 × 64 and LEHR or VXGP collimator with an

energy window of $140 \text{ keV} \pm 10\%$. The scan completed upon acquisition of 300,000 counts in the first ECG bin. Each scan took between 15 and 20 minutes. The heart occupied at least 50% of the field of view with imaging performed predominantly in the 30° - 45° position although this angle was varied outside this range when required. No caudal tilt was employed.

rP-RNV Image Processing

A custom MATLAB® program was written to import and process SPECT-RNV data. The program operates by requiring only the planar LAO projection angle and the reconstructed SPECT transaxial data. A spatial transformation was applied to each of the 16-time bins of SPECT-RNV dataset with the following conditions:

- A multi-dimensional affine spatial transform structure (N-D) which allows the rotation of the dataset by the P-RNV projection angle, θ , through the use of a 3D rotation matrix:

$$R = \begin{pmatrix} \cos(\theta) & \sin(\theta) & 0 \\ -\sin(\theta) & \cos(\theta) & 0 \\ 0 & 0 & 1 \end{pmatrix}.$$

- A resampling structure, which decides how to interpolate values over the input array at specified locations. In this work, we used nearest neighbour interpolation.

Once the SPECT-RNV dataset was rotated, each of the 16-time frames of data was summed to produce an rP-RNV dataset. The process is illustrated graphically in Figure 1. The average time taken to produce an rP-RNV DICOM file was 2.1 seconds on a standard Windows PC (2.4 GHz, 2 GB RAM). The reprojection technique did not include corrections for scatter, attenuation or distance-dependent LEHR/VXGP collimator resolution.

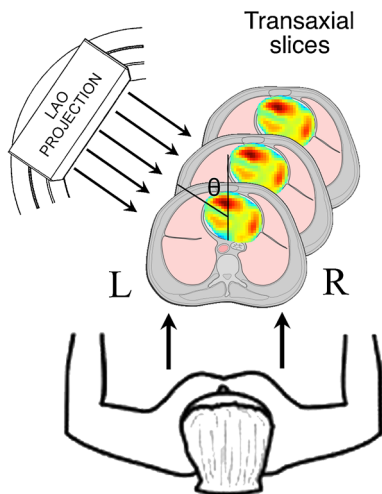


Figure 1. Graphical description of reprojection of acquired SPECT-RNV data to produce a gated planar dataset (rP-RNV) to be subsequently analysed by planar software. The data in each time bin is rotated by the angle θ and summed along this projection angle, thereby simulating an LAO acquisition.

P-RNV and rP-RNV Image Analysis: FUGA

All planar analysis (P-RNV and rP-RNV datasets) was performed using HERMES FUGA Gated Blood Pool v4.7 (Hermes Medical Systems, Stockholm, Sweden). The software uses semi-automatic edge detection using filtered data and amplitude/phase images (i.e. first and second derivatives along count density profiles), and a semi-automatically defined background region. All regions are manually adjustable. An experienced nuclear medicine physician adjusted the limiting regions where deemed necessary. The LVEF is calculated as

$$\text{LVEF} = \frac{C_{\text{ED}} - C_{\text{ES}}}{C_{\text{ED}}},$$

where C_{ED} and C_{ES} represent the background-corrected ROI counts at end-diastole and end-systole, respectively. Manually adjusted ejection fraction values for planar (EF_P) and reprojected (EF_R) were reported for each patient.

Numerical Analysis

To determine significance between pairs of techniques, paired two-tailed t tests were performed with a Bonferroni correction. The significance level was reduced from 0.05 to $0.05/3 = 0.017$ for the three tests to account for the increased chance of finding a significant result.

For a subset of 38 patients referred for cardiotoxic screening, we also examined the true positive and true negative rates of the rP-RNV technique with respect to P-RNV using the local LVEF threshold of 50%. The number of false positives ($\text{EF}_R < 50\%$, $\text{EF}_P > 50\%$), and false negatives ($\text{EF}_R > 50\%$, $\text{EF}_P < 50\%$) were also determined. These values are also provided for SPECT-RNV for completeness.

As an additional qualitative exercise, for a subset ($n = 10$) of the 47 patients the parametric data (amplitude and phase images and RWM) for rP-RNV, P-RNV and SPECT-RNV were evaluated side by side (i.e. unblinded) in order to assess qualitative clinical concordance of the techniques. EF for each technique was also re-analysed in this latter exercise. Paired t tests were performed between the EF determined from the blinded study compared to the unblinded review. The significance levels for these tests were also adjusted with a Bonferroni correction as described above. Concordance of rP-RNV with P-RNV and SPECT-RNV images was assessed via amplitude, phase and RWM images by the reporting physician.

RESULTS

All three imaging techniques were used to determine EF_P , EF_S and EF_R for each patient as described above. Figure 2 shows images from a single time bin for a single patient produced by rP-RNV and P-RNV, respectively, with lower image resolution in the rP-RNV dataset due to lower zoom and larger pixel size used in the SPECT acquisition. This is explained further in ‘Discussion’.

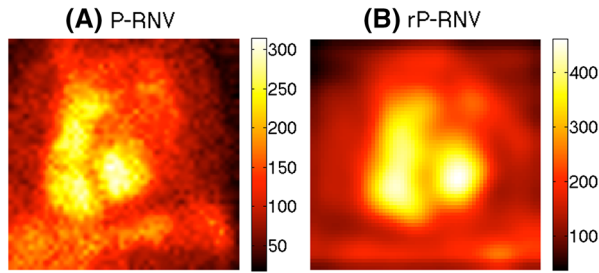


Figure 2. Comparison of the P-RNV (A) and rP-RNV (B) images for a single patient. The rP-RNV datasets are of lower resolution due to the lower zoom and larger pixel size of the SPECT study.

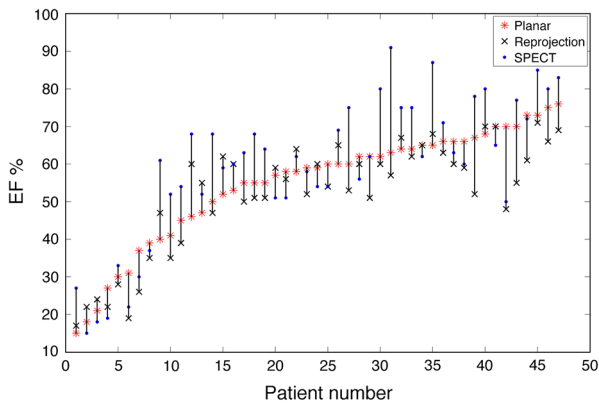


Figure 3. Graph showing the range of values of LVEF determined by EF_P , EF_R , and EF_S . The reporting physician was blinded to the results of each imaging test. Results are plotted in ascending order of EF_P .

Figure 3 shows the results of each imaging technique for each patient, showing the variation of EF% between each technique. In order to examine the difference between the individual tests post-hoc paired two-tailed *t* tests were performed between each technique with a Bonferroni correction. Results of these tests are shown in Table 2. Comparison of the ejection fractions determined by rP-RNV and SPECT-RNV to standard planar imaging is shown in Figure 4. Linear fitting showed an r^2 coefficient of 0.79 and 0.73 for EF_R vs EF_P and EF_S vs EF_P , respectively. Bland-Altman analysis between EF_P and EF_R in Figure 5A shows no bias between the LVEF determined by both techniques, the slope of the relationship was 0.02. Figure 5B shows a bias towards higher values determined by SPECT-RNV, as the slope of the linear fit was -0.2 . The plots show a standard deviation of 6.5% for P-RNV against rP-RNV, and 8.8% for P-RNV against SPECT-RNV data. The 95% confidence interval limits are 13.1% to -22.2% for SPECT-RNV against rP-RNV, and 15.6% to -9.9% for P-RNV against rP-RNV.

Table 2. Results of *t* tests between pairs of imaging techniques showing no statistical difference in ejection fraction between EF_P and EF_R and statistical difference between EF_P and EF_S and also between EF_R and EF_S

EF_P vs EF_R	$P > .017$
EF_P vs EF_S	$P < .017$
EF_R vs EF_S	$P < .017$

Thus, the bias of the SPECT-RNV technique is evident.

Assuming P-RNV as the ‘true’ imaging technique for determination of our locally defined 50% threshold for continuation of potentially cardiotoxic treatments, rP-RNV (and SPECT-RNV) can be compared in terms of analysing whether the techniques report a value above or below the threshold for each patient. Table 3 shows the results for the subset of 38 patients on potentially cardiotoxic treatments. For rP-RNV, a combined true positive and true negative rate of 35/38 patients (92.1%) was determined in reference to the P-RNV technique, while there were 2 false positive and 1 false negative. For SPECT-RNV, the combined true positive and true negative rate was 34/38 patients (89.5%), with 4 false negatives and no false positives.

For the subset of ten patients analysed with the physician unblinded, no statistical difference was observed between the blinded and unblinded ejection fractions reported for P-RNV ($P = .25$), rP-RNV ($P = .14$) and SPECT-RNV ($P = .18$). For the qualitative assessment, we scored the amplitude, phase and regional wall motion of rP-RNV in terms of clinical concordance with the corresponding P-RNV and SPECT-RNV images. These results, summarised in Table 4, show that only 1 amplitude image and 1 RWM image was not concordant with the respective P-RNV image. All phase images were clinically concordant. The rP-RNV technique was diagnostically equivalent in the majority of cases to P-RNV and SPECT-RNV. The non-equivalence with SPECT-RNV was due to inherent differences between the two techniques, principally better visualisation of apical wall motion in SPECT. Comparing with P-RNV in one case a RWM abnormality was apparent in SPECT-RNV and rP-RNV but not in planar, suggesting an advantage of reprojection over true planar. However in one case, the amplitude image mismatch between planar and reprojected, namely the loss of amplitude in the anterior wall in rP-RNV shown in Figure 6, would have altered patient diagnosis.

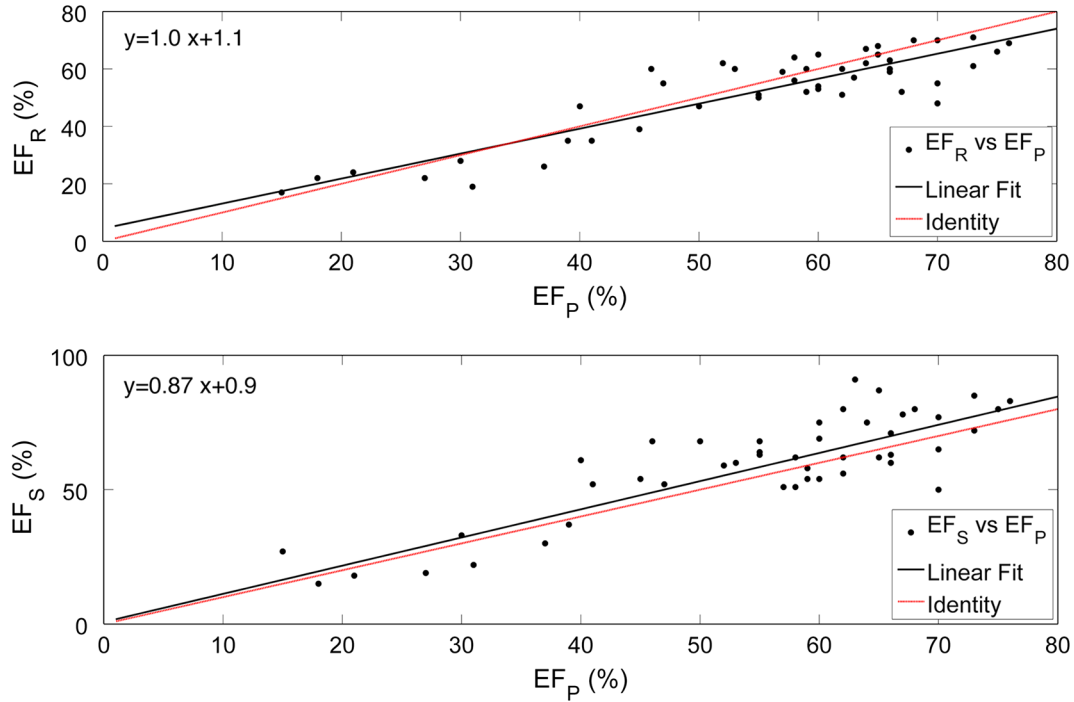


Figure 4. Graphs showing the determined relationships between EF_R and EF_S against the clinical standard of EF_P . Values of R^2 were 0.79 and 0.73 for EF_R and EF_S , respectively.

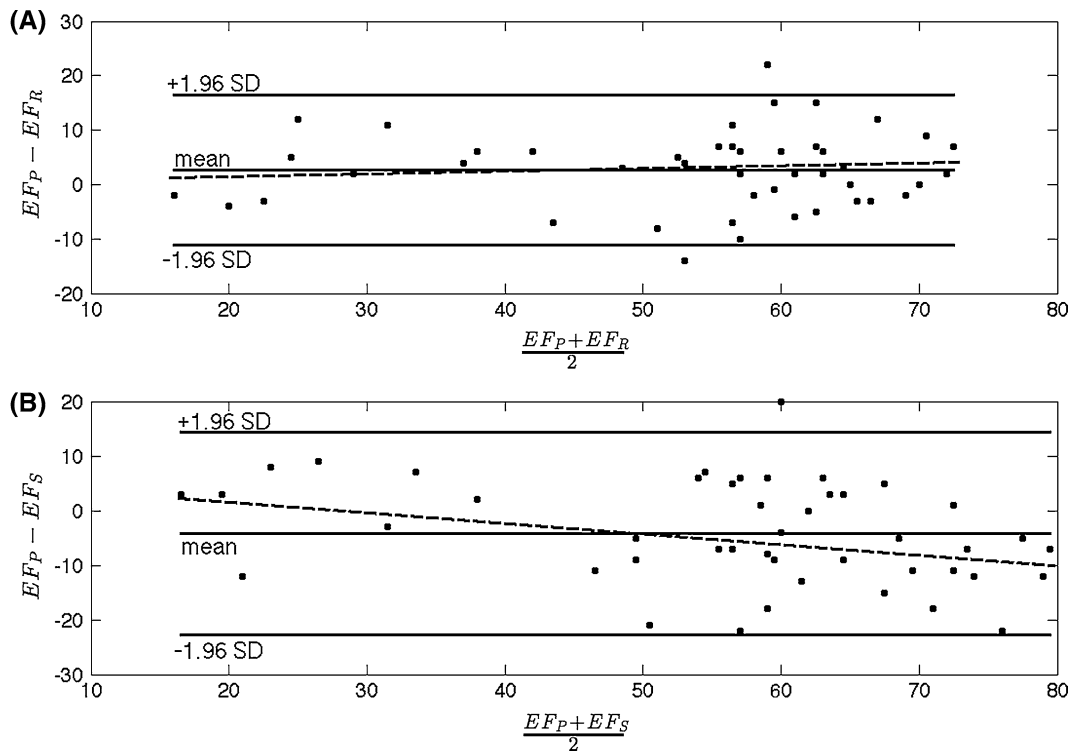


Figure 5. Bland-Altman analysis of the ejection fractions after image processing for the rP-RNV (A) and SPECT-RNV (B) techniques against P-RNV ejection fraction. The bias due to overestimation of the SPECT-RNV (EF_S) can be observed in (B).

Table 3. Comparison of the techniques in terms of identifying the correct side of the 50% threshold of LVEF when compared to P-RNV

	SPECT-RNV	rP-RNV
True positives and true negatives	34	35
False positives	0	2
False negatives	4	1

False positive indicates that the technique calculated the EF < 50% threshold (when P-RNV > 50%), and false negative indicating that the technique calculated the EF to be >50% (when P-RNV < 50%).

Table 4. Diagnostic equivalence of amplitude, phase and regional wall motion images of the 10 patients assessed between rP-RNV and P-RNV/SPECT-RNV

Comparison of techniques	Amplitude	Phase	RWM
rP-RNV vs P-RNV	9/10	10/10	9/10
rP-RNV vs SPECT-RNV	9/10	8/10	9/10

rP-RNV images were scored in terms of concordance with the P-RNV and SPECT-RNV images.

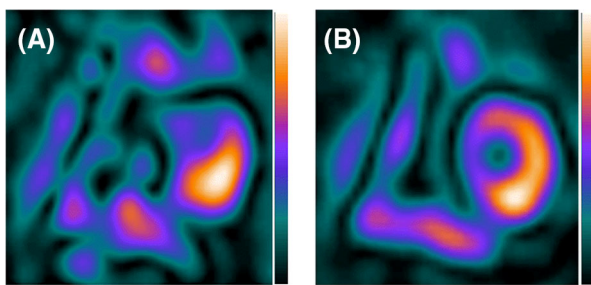


Figure 6. rP-RNV (A) and P-RNV (B) amplitude images showing loss of amplitude in the anterior wall, which would have altered the patient diagnosis.

DISCUSSION

It should be noted that correlation to the current imaging clinically accepted standard of P-RNV, while valuable, remains confounded given the limitations of P-RNV that have been well documented and investigated.^{7,17,18} Much work has been done to improve the standing of SPECT-RNV, from improved algorithms and software to scanning technique. Studies have also attempted to use cardiac magnetic resonance imaging (C-MRI) as a more accurate imaging gold standard.¹⁹⁻²¹ However, we employed P-RNV as the gold standard due to its clinical reliability, ease of implementation and use in many nuclear medicine departments worldwide for many years.

Recent work comparing reprojected SPECT from a dedicated CZT cardiac imaging system against P-RNV acquired from two different traditional NaI systems (one cardiac specific, the other a general dual-headed

system)¹⁶ showed correlation of $r > 0.94$. It should be noted that there remains significant differences in the imaging systems in terms of detector technology and system operation. Our work combined SPECT-RNV followed immediately by P-RNV without movement of the patient on the same gamma camera, thereby reducing possible errors associated with imaging on different instrumentation.

Differences arise between the resulting clinical images from the techniques described in this work. The lower zoom and larger pixel size used in the SPECT studies reduces the effective final image resolution. Thus as the rP-RNV images are generated from reprojection of the SPECT-RNV datasets, they also suffer from the same lower resolution. This effect can be observed clearly in Figure 2, and interpolation of SPECT data also serves to compromise the resolution.

59% of results showed an overestimation of EF% measured by SPECT-RNV over P-RNV, whereas only 15% of rP-RNV values were greater than P-RNV. This overestimation of SPECT-RNV compared to P-RNV can be observed in Figure 3, this has been well documented by other work.^{7,10,18,22} This is also shown in the *t* tests shown in Table 2 where the means of EF_S and EF_P are shown to be statistically different. A linear relationship between EF_R and EF_P ($r^2 = 0.79$) and between EF_R and EF_S ($r^2 = 0.73$) can be observed in Figure 4, showing that results from each imaging technique are comparable and are close to the line of identity. These correlation values compare well to others comparing SPECT and planar LVEF values on NaI cameras.^{7,22} Bland-Altman plots in Figure 5 show the

variation in EF_R and EF_S compared to EF_P . As found in other work, SPECT-RNV produces higher LVEF values than planar at the higher end of the LVEF range as indicated by the slope of linear regression in Figure 5B (slope = -0.2). The relationship is not true for the rP-RNV LVEF values where the slope is much closer to zero (slope = 0.02). Reasons for this overestimation have been investigated previously and are caused mainly by left atrial overlap in the planar studies which are not present in the SPECT-RNV dataset, as well as partial volume effects. The 95% confidence limits shown in Figure 5 between SPECT-RNV and P-RNV are consistent with other works employing traditional dual-headed NaI gamma cameras for SPECT-RNV (95% limits of 19.5% and -32.5% ,¹² 11% and -22% ,²³ 15% and -15% ²⁴). Figure 5 also shows a standard deviation of 7%, which is slightly larger than the 5% error associated with conventional P-RNV. A larger patient population may help to further reduce the standard deviation associated with the P-RNV and rP-RNV comparison.

For one of our subjects, it was noted that an EF_S of 91% corresponded to an EF_P and EF_R of 63% and 57%, respectively. SPECT-RNV may not possess the ability to track a ventricle that contracts to a small volume in systole, therefore partial volume effects may cause an overestimation of the EF compared to planar. Thus in this case the rP-RNV EF provides a more robust assessment of the EF, and is similar to the P-RNV EF.

Statistical differences in EF between 8 and 16-frame P-RNV have been noted in previous work.²⁵ In our work we used 16 frames, which has been determined as adequate for LVEF determination by European guidelines.⁹ Although 24–32 frames is preferred by the American Society of Nuclear Cardiology (ASNC) for planar imaging (in order to increase the accuracy of the variable associated with imaging),⁸ for imaging with traditional NaI cameras this adjustment will also increase the imaging time.

SPECT-RNV imaging time was similar to that of a planar scan. It is important that enough data be acquired to reduce the possibility of not being able to automatically determine the SPECT-RNV volumes due to poor counting statistics. There were approximately 7 times more counts in the reconstructed SPECT-RNV datasets (mean = 39.12×10^6) than in P-RNV (mean = 5.69×10^6 counts) datasets. All the acquired counts in the SPECT study are used in the formation of each rP-RNV image. However, in order to create a rP-RNV dataset with a similar volume of the FoV occupied by the heart as P-RNV data, the SPECT datasets were cropped. After cropping, there were more counts on average in the rP-RNV than in P-RNV (8.57×10^6 and 5.69×10^6 counts, respectively) datasets. It is important to maintain similar count statistics to the P-RNV dataset

due to FUGA software using count density profiles in the segmentation of the LV volume.

Standardisation of SPECT image reconstruction is also important in terms of comparison of datasets. The cutoff frequency of the reconstruction filter, in the range of $0.30\text{--}0.45$ cycles- cm^{-1} , has been shown to have a minimal effect on the correlation to P-RNV results, yet it has been seen to affect the bias.²² In this work, all SPECT data were reconstructed on one system thereby standardising the SPECT-RNV data from both gamma cameras.

Clinically in terms of continuation of cardiotoxic drug treatment, an incipient fall in LVEF detected on serial RNV provides an appropriate and cost-effective approach for predicting and preventing impending congestive heart failure. Patients with a normal baseline LVEF ($\geq 50\%$) and a 10% or greater point fall in LVEF to a final value of less than 50% during doxorubicin therapy are considered 'at risk' for congestive heart failure.²⁶ It may transpire that because of elevated EF when reporting SPECT EF, due to the removal of regional impairment, these threshold values may need to be revised.

Table 3 shows the rate of true positive and negative cases for the rP-RNV technique compared to the P-RNV technique with a high rate of agreement. Although there was a high rate of agreement in terms of the 50% threshold, there were 2 false positive and 1 false negative cases. It should be noted that for these three cases EF_R differed from EF_P by less than 5 EF%, which is within the reproducibility of P-RNV. For completeness, SPECT-RNV results are also presented, with four false negatives. The lack of false positive results again shows the bias of the SPECT-RNV technique, which may be resolved by using the reprojected dataset.

Out of the subset of ten patients presented in Table 4, P-RNV and rP-RNV were assessed as non-diagnostically equivalent in only 1 amplitude image (Figure 6) and also in 1 RWMA image. All phase images were assessed as diagnostically equivalent. rP-RNV was also able to highlight septal asynchrony which was not observed on the P-RNV image. Slightly more differences existed in SPECT-RNV imaging, 1 amplitude image, 2 phase images and 2 RWMA images. Certain issues were highlighted that were due to fundamental differences in the imaging techniques; for example in one case apicoseptal hypokinesis was identified from the SPECT-RNV amplitude and RWMA images, however, owing to the degeneracy of P-RNV and rP-RNV these latter techniques showed apical hypokinesis only. SPECT-RNV showed a loss of phase in the lateral wall, which could not be seen in P-RNV and rP-RNV images. These results, coupled with the results of *t* tests for the entire 47 patient dataset show

that rP-RNV can be considered a good substitute to standard P-RNV, although like all other imaging techniques, caution should be exercised in interpreting its results.

LIMITATIONS OF STUDY

Our work did not include corrections for attenuation or scatter, however we only used 180° acquisition for the SPECT-RNV dataset in order to avoid posterior projections, which serve to increase noise due to significant attenuation and decreased image resolution due to increased distance from the detectors. A gated transmission scan can be used for attenuation correction, however, previous SPECT-RNV work has shown no significant difference between attenuation corrected and non-corrected LVEF.²⁷ The capability of performing transmission scans is also a declining feature on modern gamma cameras.

A cine CT which covers multiple phases of the cardiac cycle may also be used to correct the SPECT data, although this technique may not be favoured due to the higher radiation dose given to the patient. The use of a standard non-gated CT scan has had mixed effects,²⁸ in some cases leading to lower LVEF.²⁹ This work also notes that the attenuation correction by single CT provides little extra benefit for the extra radiation dose, and its acquisition has since been discontinued.

Recent work has shown that a triple-energy window scatter correction, along with generation of attenuation coefficient maps from the scatter images can provide increases in sensitivity in the left anterior descending artery territory and specificity in the right coronary artery territory for myocardial perfusion studies.³⁰ Such methodology would be easily adapted to RNV studies. Unfortunately as our work was a retrospective study without the acquisition of scatter windows, attenuation coefficient maps could not be generated. Accounting for attenuation may increase the intensity of the blood pool in the images and owing to the relatively large volume of the LV, attenuation correction may affect the volume of the shape fitted to the LV (as the algorithm is count dependent), as is noted in previous work.²⁹ A study on the effects of attenuation correction of SPECT-RNV is part of our future plans.

The independent contributions of partial volume and left atrial overlap are difficult to quantify in clinical cases, this would warrant further local studies with controlled phantom experiments where the LV size could be adjusted to a range of clinically relevant volumes. It may also be possible to mask the left atrium in the reconstructed SPECT images prior to reprojection. Subtraction of the EF calculated with and without atrial contribution would quantify the effect.

Variability may have been affected in the study by the fact that our work comprised of patients with a range of referral criteria, from cardiotoxic assessment to atrial fibrillation and cardiac resynchronization therapy. Pacing induces ventricular dys-synchrony and this may have impaired the repeatability between the concurrent P-RNV and SPECT-RNV measurements in this study. Further study on the reproducibility of the rP-RNV technique should also be carried out on a larger patient dataset.

NEW KNOWLEDGE GAINED

Although the left ventricular ejection fraction determined by SPECT-RNV can be consistently higher than values provided by planar imaging, reprojection of the SPECT dataset to a 'pseudo-planar' provides LVEF values statistically equivalent to the planar data.

CONCLUSION

We have performed P-RNV followed immediately by SPECT-RNV on 47 patients, and using a reprojection technique of the SPECT dataset, provided a further evaluation technique for measuring LVEF which is statistically equivalent to the LVEF provided by standard planar imaging. Thus, standard planar imaging can be supplanted by a combination of the SPECT-RNV and rP-RNV techniques.

Acknowledgments

The authors are grateful to the radiography staff at the Department of Nuclear Medicine, Royal Brompton Hospital for their help in data collection. JOD acknowledges financial support from the Department of Health via the National Institute for Health Research (NIHR) comprehensive Biomedical Research Centre award to Guy's & St Thomas' NHS Foundation Trust in partnership with King's College London and King's College Hospital NHS Foundation Trust and The Centre of Excellence in Medical Engineering funded by the Wellcome Trust and EPSRC under Grant Number WT088641/Z/09/Z. The views expressed are those of the author(s) and not necessarily those of the NHS, the NIHR, the DoH, EPSRC, or Wellcome Trust.

Disclosure

The authors have nothing to disclose.

References

1. Habash-Bseiso DE, Rokey R, Berger C, Weier AW, Chyou PH. Accuracy of noninvasive ejection fraction measurement in a large community-based clinic. *Clin Med Res* 2005;3:75-82.
2. Wackers FJ, Berger HJ, Johnstone DE, Goldman L, Reduto LA, Langou RA, et al. Multiple gated cardiac blood pool imaging for left ventricular ejection fraction: Validation of the technique and assessment of variability. *Am J Cardiol* 1979;43:1159-66.

3. Strauss HW, Zaret BL, Hurley PJ, Natarajan TK, Pitt BA. Scintiphotographic method for measuring left ventricular ejection fraction in man without cardiac catheterization. *Am J Cardiol* 1971;28:575-80.
4. Bhullar N, Walker J, Lytwyn M, Jassal D. The role of cardiac MRI for serial assessment of left ventricular ejection fraction in breast cancer patients. *J Cardiovasc Magn Reson* 2010;12:198.
5. White HD, Brown MA, Brandt PW, Whitlock RM, Wild CJ. Left ventricular end-systolic volume as the major determinant of survival after recovery from myocardial infarction. *Circulation* 1987;76:44-51.
6. Nichols KJ, Watson DD. The motivation to reproject gated blood pool SPECT data as planar data. *J Nucl Cardiol* 2013;20:329-30.
7. Bartlett ML, Srinivasan G, Barker WC, Kitsiou AN, Dilsizian V, Bacharach SL. Left ventricular ejection fraction: Comparison of results from planar and SPECT gated blood-pool studies. *J Nucl Med* 1996;37:1795-9.
8. Corbett JR, Akinboboye OO, Bacharach SL, Borer JS, Botvinick EH, DePuey EG, et al. ASNC imaging guidelines for Nuclear Cardiology procedures: Equilibrium radionuclide angiocardiology. *J Nucl Cardiol* 2006;13:e56-79.
9. Hesse B, Lindhardt TB, Acampa W, Anagnostopoulos C, Ballinger J, Bax JJ, et al. EANM/ESC guidelines for radionuclide imaging of cardiac function. *Eur J Nucl Med Mol Imaging* 2008;35:851-85.
10. Eder V, Bernis F, Drumm M, Diarra MI, Bailieu F, Léger C. Three-dimensional analysis of left ventricle regional wall motion by using gated blood pool tomography. *Nucl Med Commun* 2004;25:971-8.
11. Adachi I, Akagi H, Umeda T, Suwa M, Komori T, Ogura Y, et al. Gated blood pool SPECT improves reproducibility of right and left ventricular Fourier phase analysis in radionuclide angiography. *Ann Nucl Med* 2003;17:711-6.
12. Daou D, Coaguila C, Benada A, Razzouk M, Haidar M, Colin P, et al. The value of a completely automatic ECG gated blood pool SPECT processing method for the estimation of global systolic left ventricular function. *Nucl Med Commun* 2004;25:271-6.
13. Van Kriekinge SD, Berman DS, Germano G. Automatic quantification of left ventricular ejection fraction from gated blood pool SPECT. *J Nucl Cardiol* 1999;6:498-506.
14. De Bondt P, Nichols K, Vandenberghe S, Segers P, De Winter O, Van de Wiele C, et al. Validation of gated blood-pool SPECT cardiac measurements tested using a biventricular dynamic physical phantom. *J Nucl Med* 2003;44:967-72.
15. Groch MW, DePuey EG, Belzberg AC, Erwin WD, Kamran M, Barnett CA, et al. Planar imaging versus gated blood-pool SPECT for the assessment of ventricular performance: A multicenter study. *J Nucl Med* 2001;42:1773-9.
16. Vanhove C, Franken PR, Defrise M, Momen A, Everaert H, Bossuyt A. Automatic determination of left ventricular ejection fraction from gated blood-pool tomography. *J Nucl Med* 2001;42:401-7.
17. Nichols K, Humayun N, DeBondt P, Vandenberghe S, Akinboboye OO, Bergmann SR. Model dependence of gated blood pool SPECT ventricular function measurements. *J Nucl Cardiol* 2004;11:282-92.
18. Wells RG, Marvin B, Kovalski G, Ruddy T. Planar radionuclide angiography with a dedicated cardiac SPECT camera. *J Nucl Cardiol* 2013;20:358-66.
19. Godkar D, Bachu K, Dave B, Megna R, Niranjana S, Jhanna A. Comparison and co-relation of invasive and noninvasive methods of ejection fraction measurement. *J Natl Med Assoc* 2007;99:1227-34.
20. Harel F, Finnerty V, Ngo Q, Grégoire J, Khairy P, Thibault B. SPECT versus planar gated blood pool imaging for left ventricular evaluation. *J Nucl Cardiol* 2007;14:544-9.
21. Nichols K, Saouaf R, Abaneh AA, Barst RJ, Rosenbaum MS, Groch MW, et al. Validation of SPECT equilibrium radionuclide angiographic right ventricular parameters by cardiac magnetic resonance. *J Nucl Cardiol* 2002;9:153-60.
22. Xie BQ, Tian YQ, Zhang J, Zhao SH, Yang MF, Guo F. Evaluation of left and right ventricular ejection fraction and volumes from gated blood-pool SPECT in patients with dilated cardiomyopathy: Comparison with cardiac MRI. *J Nucl Med* 2012;53:584-91.
23. Jensen MM, Schmidt U, Huang C, Zerahn B. Gated tomographic radionuclide angiography using cadmium-zinc-telluride detector gamma camera; comparison to traditional gamma cameras. *J Nucl Cardiol* 2014;21:384-96.
24. Wright GA, Thackray S, Howey S, Cleland JG. Left ventricular ejection fraction and volumes from gated blood-pool SPECT: Comparison with planar gated blood-pool imaging and assessment of repeatability in patients with heart failure. *J Nucl Med* 2003;44:494-8.
25. Kim SJ, Kim IJ, Kim YS, Kim YK. Gated blood pool SPECT for measurement of left ventricular volumes and left ventricular ejection fraction comparison of 8 and 16 frame gated blood pool SPECT. *Int J Cardiovasc Imaging* 2005;21:261-6.
26. Mitani I, Jain D, Joska TM, Burtness B, Zaret BL. Doxorubicin cardiotoxicity: Prevention of congestive heart failure with serial cardiac function monitoring with equilibrium radionuclide angiocardiology in the current era. *J Nucl Cardiol* 2003;10:132-9.
27. Sundram F, Notghi A, Deakin A. Does attenuation correction of gated tomographic cardiac blood pool studies affect left ventricular volumes and ejection fraction values? *Nucl Med Commun* 2006;27:A47.
28. Seierstad T, Bogsrud T, Skretting A. Effects of photon attenuation on the determination of cardiac volumes from reconstructed counts in gated blood pool SPET. *Eur J Nucl Med Mol Imaging* 2003;31:399-402.
29. Sibille L, Bouallegue FB, Bourdon A, Mariano-Goulard D. Influence of CT-based attenuation correction in assessment of left and right ventricular functions with count-based gated blood-pool SPECT. *J Nucl Cardiol* 2011;18:642-9.
30. Yamauchi Y, Kanzaki Y, Otsuka K, Hayashi M, Okada M, Nogi S, et al. Novel attenuation correction of SPECT images using scatter photopeak window data for the detection of coronary artery disease. *J Nucl Cardiol* 2014;21:109-17.